ABCM Symposium Series in Mechatronics - Vol. 2 - pp.469-476

DESIGN OF ELECTROTHERMOMECHANICAL MEMS

Wilfredo Montealegre Rubio
University of São Paulo, Av. Prof. Mello Moraes, 2231 - Cidade Universitária, São Paulo – SP, Brazil
wilfredo.rubio@poli.usp.br

Paulo Henrique de Godoy
University of São Paulo, Av. Prof. Mello Moraes, 2231 - Cidade Universitária, São Paulo – SP, Brazil
pegodoy@uol.com.br

Emílio Carlos Nelli Silva
University of São Paulo, Av. Prof. Mello Moraes, 2231 - Cidade Universitária, São Paulo – SP, Brazil
ecnsilva@usp.br

Abstract. *A very common type of MEMS (MicroElectroMechanical Systems) are the electrothermomechanical MEMS which couples electrical, thermal and mechanical field to generate displacements. In these MEMS an electrical current is converted to heat by Joule's heating and the heat causes thermal strain, which in turn causes structural deformation. Electrothermomechanical MEMS are designed as compliant mechanisms; they attain their mobility from flexibility of their structure as opposed to rigid body structure that attains their mobility from hinges, bearings and sliders. Design of electrothermomechanical MEMS is not an easy task to be accomplished by using trial and error methods, therefore, in this work Topology Optimization Method is applied, which combines optimization algorithms with Finite Element Method to design the best structure topology, distributing the material in the interior of a fixed domain according to cost criteria. In electrothermomechanical MEMS, this cost criteria consists of maximizing the output displacement, with the least weight, when an electric potential is applied to the structure. The main goal of this work is to design eletrothermomechanical MEMS using the Topology Optimization Method. A material model based on the traditional SIMP model is adopted and the optimization algorithm is constructed based on sequential linear programming (SLP). A filtering technique is applied to control the mesh dependency and the checkerboard problem. To illustrate the method, several examples of optimized two-dimensional eletrothermomechanical MEMS are included. In addition, the influence of different values of optimization parameters upon the final topology is discussed.*

Keywords*: Eletrothermomechanical MEMS, compliant mechanisms, design, topology optimization, finite element method, microactuators.*

1. Introduction

Micromechanisms are microscopic mechanical systems with feature sizes ranging from micrometers to millimeters. Micromechanisms are also named MEMS (MicroEletroMechanical Systems). They may be manufactured using methods similar to those applied to construct integrated circuits, and their size also makes possible to integrate them into a wide range of systems, such as microsensors – e.g. accelerometers for air-bag; micropumps (Lintel *et al.*, 1988); medical instruments for in-body surgery, microgrippers (Larsen *et al.*, 1997) and positioning microrobotic devices (Sigmund, 2001a). Because of the small scale, micromechanisms are designed without hinges and bearings as seen in conventional mechanisms, they are designed as compliant mechanisms (Howell, 2001) which gain their mobility from the deflection of flexible members rather that from movable joints.

The main actuation principles for compliant micromechanisms are electrostatics, electrothermal, electromagnetic, piezoelectric, and shape memory. In the electromechanical actuation principle an input electrical current is converted to heat by Joule's heating and the heat then causes thermal strain, which in turn causes structural deformation, see Fig. 1a. Due to the complexity of these multiphysics problems, many compliant micromechanisms actuated electro-thermally, also named electrothermomechanical MEMS, are designed using intuition, experience and trial and error approaches. A typical example these actuators are called 'U-shaped' actuators (Chen *et al.*, 2002; Moulton and Ananthasuresh, 2000; Comtois *et al.*, 1998), shown in Fig. 1b. The device is composed of two suspended beams with variable cross sections joined at the free end, which constrains the tip to move in an arcing motion while current is passed through the actuator. Commonly, this actuator is named Guckel actuator (Guckel, 1992). Other popular intuitive electrothermal actuator is called 'V-shaped' characterized by an axial displacement (Chu *et al.*, 2003), see Fig. 1a. However, only with Sigmund's papers (2001a and 2001b) was introduced a systematic tool for design of planar micromechanisms actuated electro-thermally based on continuum topology optimization. Ananthasuresh (2003) designed electrothermomechanical MEMS using topology optimization based on truss and beam finite elements.

Topology optimization is a powerful structural optimization method that combines a numerical solution method, usually the Finite Element Method (FEM), with an optimization algorithm to find an optimal material distribution inside a given domain (Bendsøe and Sigmund, 2003). Since their introduction (Bendsøe and Kikuchi, 1988) topology optimization methods have been successfully used in numerous applications, including design of materials (Bendsøe and Sigmund, 2003), mechanisms (Nishiwaki *et al.*, 1998, Silva *et al.* 1997), MEMS and many other structural design

problems (Bendsøe and Sigmund, 2003). Topology optimization is a systematic and powerful tool for complex multiphysics design problems, including electrothermomechanical MEMS, which searches a structural topology that maximizes a desired displacement generated when an input electric potential is applied over the structure

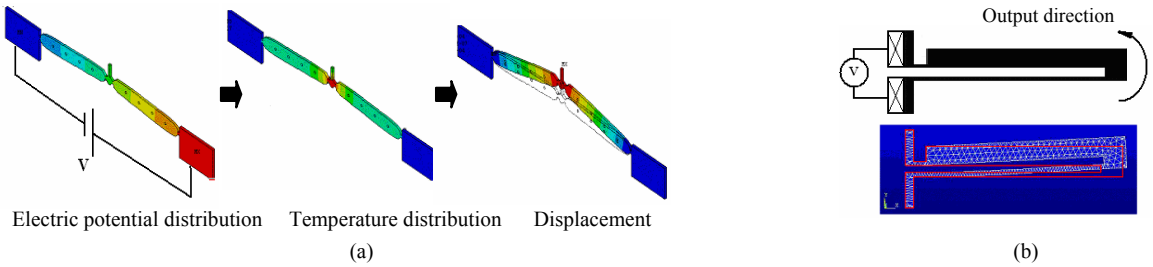

Figure 1.Typical examples of intuitive electrothermomechanical MEMS. a) 'V-shaped' actuator and electrothermomechanical actuation principle; b) Guckel actuator and simulation.

In this paper, it will be designed electrothermomechanical MEMS using continuum type topology optimization. A material interpolation scheme based on the traditional SIMP model is adopted and the optimization algorithm is constructed based on sequential linear programming (SLP). A spatial filtering technique and 4-node quadrilateral finite elements are used. Examples of two-dimensional eletrothermomechanical MEMS designed using the implemented method are presented. In addition, the influence of different values of optimization parameters upon the final topology as material volume constraint and mesh refinement of finite element is discussed.

The paper is built up as follow. Section 2 describes the FEM formulation for eletrothermomechanical MEMS. In Section 3 the topology optimization formulation for electrothermomechanical MEMS design is discussed and the sensitivity analysis. In Section 4 some results are presented. Finally, in Section 5 some conclusions are given.

2. Electrothermomechanical FEM formulation

Electrothermomechanical MEMS work in several energy fields: electric field, thermal field and elastic field (Mankame and Ananthasuresh, 2001). Thus, a electrothermomechanical FEM modeling includes three stages: electrical analysis to determine the voltages distribution, thermal analysis to determine the temperature distribution by Joule's heating, and elastic deformation analysis in the presence of thermal loads.

A linear FEM formulation is applied, therefore, only small displacements are considered and the three FEM analyses can be carried out sequentially without considering temperature dependence of electrical, thermal, and elastic properties. The two-dimensional design domain is assumed to be rectangular and it is discretized by means of 4-node quadrilateral finite elements, and it assumes plane stress state. The three finite elements problems are (Sigmund, 2001a):

$$\boldsymbol{K}_0(\rho)\boldsymbol{U}_0(\rho) = \boldsymbol{P}_0 \quad \Rightarrow \quad \textbf{Electrical Analysis} \tag{1}$$

$$\boldsymbol{K}_1(\rho)\boldsymbol{U}_1(\rho) = \boldsymbol{P}_1(\boldsymbol{U}_0(\rho), \rho) \quad \Rightarrow \quad \textbf{Thermal Analysis} \tag{2}$$

$$\boldsymbol{K}_2(\rho)\boldsymbol{U}_2(\rho) = \boldsymbol{P}_2(\boldsymbol{U}_1(\rho), \rho) \quad \Rightarrow \quad \textbf{Elastic Analysis} \tag{3}$$

where, index 0, 1, 3 refer to electrical, thermal and elastic analyses, respectively. The number of elements used in the discretization is N and n is the number of nodes. $\boldsymbol{K_o}$ and $\boldsymbol{K_1}$ (n x n – one degrees of freedom per node) are global electrical and thermal conductivity matrices, respectively and, $\boldsymbol{K_2}$ ($2n$ x $2n$ – two degrees of freedom per node) is global stiffness matrix. $\boldsymbol{U_o}$ and $\boldsymbol{U_1}$ (n) are the voltage and temperature output vectors, respectively, and $\boldsymbol{U_2}$ ($2n$) is the displacements output vector. $\boldsymbol{P_o}$, $\boldsymbol{P_1}$ and $\boldsymbol{P_2}$ are the electrical, thermal and structural load vectors, respectively. $\boldsymbol{\rho}$ is the density vector, which contains the design variables as defined by SIMP material model (see Section 3).

The global electrical thermal conductivity matrices and the global stiffness matrix are defined as:

$$\boldsymbol{K}_0(\boldsymbol{\rho}) = \sum_{e=1}^{N} \boldsymbol{k}_0^e(\rho^e) = \sum_{e=1}^{N} \sigma_0(\rho^e) \int_{V^e} \boldsymbol{B}_0^T \boldsymbol{B}_0 \, dV \tag{4}$$

$$\boldsymbol{K}_1(\boldsymbol{\rho}) = \sum_{e=1}^{N} \left(\boldsymbol{k}_1^e(\rho^e) + \boldsymbol{h}^e\right) = \sum_{e=1}^{N} \sigma_1(\rho^e) \int_{V^e} \boldsymbol{B}_0^T \boldsymbol{B}_0 \, dV + \sum_{e=1}^{N} \gamma \int_{S^e} \boldsymbol{N}_0^T \boldsymbol{N}_0 \, dS \quad \text{and} \tag{5}$$

$$\boldsymbol{K}_2(\boldsymbol{\rho}) = \sum_{e=1}^{N} \boldsymbol{k}_2^e(\rho^e) = \sum_{e=1}^{N} \int_{V^e} \boldsymbol{B}_2^T \boldsymbol{D}(\rho^e) \boldsymbol{B}_2 \, dV \tag{6}$$

if m is the number of degrees of freedom (*d.o.f.*) of element e: $\boldsymbol{k}_0^e$, $\boldsymbol{k}_1^e$ (m x m) are the element electrical and thermal conductivity matrices, respectively, $\boldsymbol{h}^e$ (m x m) is the element convection matrix and, $\boldsymbol{k}_2^e$ ($2m$ x $2m$) is the element

stiffness matrix. ρ^e is the element density function (see Section 3). $\sigma_0(\rho^e)$, $\sigma_t(\rho^e)$, and γ are electrical, thermal conductivity and convection coefficient, respectively. $\boldsymbol{B}_0$ and $\boldsymbol{B}_1$ are voltage or temperature gradient and strain-displacement matrices, respectively. $\boldsymbol{D}$ is material matrix; $\boldsymbol{N}_0$ is shape functions vector, and V^e is the element volume.

In the same way, the global load vectors of thermal and elastic analysis are assembled from element load vectors:

$$\boldsymbol{P}_1(\boldsymbol{U}_0(\rho),\rho) = \sum_{e=1}^{N} \boldsymbol{p}_1^e\left(\boldsymbol{u}_0^e\left(\rho^e\right),\rho^e\right) \tag{7}$$

$$\boldsymbol{P}_2(\boldsymbol{U}_1(\rho),\rho) = \sum_{e=1}^{N} \boldsymbol{p}_2^e\left(\boldsymbol{u}_1^e\left(\rho^e\right),\rho^e\right) \tag{8}$$

where, $\boldsymbol{p}_1^e$ and $\boldsymbol{p}_2^e$ are element load vectors of thermal and elastic analysis, respectively, which depend of element voltage ($\boldsymbol{u}_0^e$) and temperature ($\boldsymbol{u}_1^e$) vectors and the element density function (ρ^e).

3. Topology optimization formulation for electrothermomechanical MEMS

Topology optimization is a powerful structural optimization technique that combines the Finite Element Method (FEM) with an optimization algorithm to find the optimal material distribution inside a given domain bounded by supports and applied loads that must contain the unknown structure (Bendsøe and Sigmund, 2003). The objective of topology optimization is to determine the holes and connectivities of the structure by adding and removing material in the extended fixed domain. The finite element model domain is not changed during the optimization process, which makes easy the calculation of derivatives of any function defined over the extended domain.

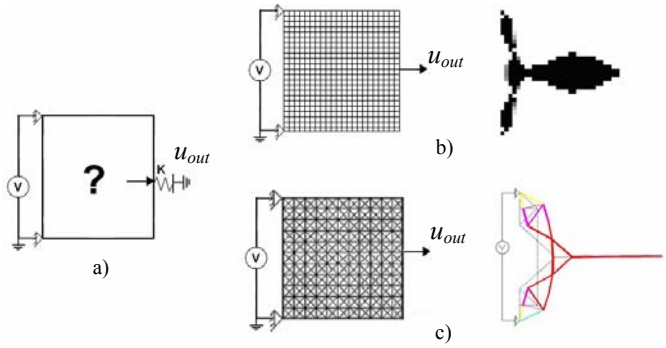

Figure 2. Electrothermomechanical MEMS design. a) Design domain; b) continuum topology optimization and optimal result; (c) grid-like (beam or truss elements) topology optimization and final result deformed.

Topology optimization is based on two main concepts: the extended design domain and the relaxation of the design domain. The extended design domain is a large fixed domain that must contain the whole structure to be determined by the optimization procedure including supports and loads applied, see Fig. 2a. The relaxation of the design domain allows the material to assume intermediate property values during the optimization procedure. It is required due to discrete material distribution function (0-1), which generates a discontinuous, ill-posed problem and difficulties in its numerical treatment due to multiple local minimums. The relaxation of the design domain is defined by a material model, which allows the material change from zero to one; see (Bendsøe and Sigmund, 1999) for a review.

In electrothermomechanical MEMS design mainly, the SIMP (Solid Isotropic Material with Penalization) material model (Sigmund, 2001a and 2001b) and peak-function material interpolation model (Ananthasuresh, 2003) are used; however in this work, the topology optimization formulation employs the material model based on the SIMP method.

The electrothermomechanical SIMP material model consists in three mathematical equations that states in each point of the domain the local effective material properties as:

$$\sigma_0\left(\rho^e\right) = \left(\rho^e\right)^p \sigma_{0_{base}}; \quad \sigma_1\left(\rho^e\right) = \left(\rho^e\right)^p \sigma_{1_{base}}; \quad E\left(\rho^e\right) = \left(\rho^e\right)^p E_{base} \tag{9}$$

σ_{0base}, σ_{ibase}, are electrical, thermal conductivity of solid material, respectively, and E_{base} is the Young's modulus of solid material. p_1, p_2, p_3 are penalization powers to recover the discrete nature of the design; in this work it uses the powers $p_1 = p_2 \geq 2$ for the conductivities and $p_3 \geq 3$ for the Young's modulus Sigmund, (2001a). ρ^e is a design variable of element e describing the amount of material in each point of the domain, which can assume values between 0 and 1. For ρ^e equal to 0, the material is equal to void and for ρ^e equal to 1 the material is equal to solid material. The convection coefficient (γ) is assumed to be independent of the element density; otherwise, low-density elements would not be cooled.

3.1. Design problem formulation

The design objective is to determine the topology of the structure that fits within a design domain and deforms as desired when subject to electrical, thermal, and mechanical boundary conditions as shown in Fig. 2a (Ananthasuresh, 2003). In electrothermomechnical MEMS design kinematics and structural requirements are implemented. Kinematics requirements consist of maximizing the output displacement (u_{out}) when an input electrical potential is applied, see Fig 2a. Structural requirements consist of maximizing the structural stiffness when an electrothermomechanical MEMS actuate on a worpiece of given stiffness. This requirement is implemented using a spring of stiffness K, see Fig. 2a. This spring is also a control to design stiff or soft electrothermomechanical MEMS.

In this work, a continuum topology optimization is used as shown in Fig. 2b, however a grid-like (beams or truss systems) topology optimization also can be used (Ananthasuresh, 2003; Rubio *et al.*, 2004), see Fig. 2c. Considering the FEM formulation for the discretized domain, the general form of the topology optimization problem for electrothermomechanical MEMS design can be defined as:

$$\begin{aligned}
&\max_{\boldsymbol{\rho}} \sum_{i=1}^{dof} u_{out} \qquad \text{(Output displacement)} \\
&\textbf{s.t.} \quad \sum_{e=1}^{N} \rho^e V^e \le V^* \ \text{(Material volume constraint)} \\
&\quad \mathbf{0} < \boldsymbol{\rho}_{\min} \le \boldsymbol{\rho} \le \mathbf{1} \\
&\quad \text{Equilibrium equations – see equations (1) up to (3)} \\
&\quad \text{Filtering technique}
\end{aligned} \tag{10}$$

where, V^* is the constraint on material volume and *d.o.f.* the degrees of freedom of the microactuator. A lower bound $\boldsymbol{\rho}_{\min}$ is also specified for design variables $\boldsymbol{\rho}$ to avoid numerical problems as singularities of the electrical and thermal conductivity matrices, and singularities of the stiffness matrix. In this work, $\boldsymbol{\rho}_{\min}$ is chosen to be 10^{-4}. Thus numerically, regions with $\boldsymbol{\rho}=\boldsymbol{\rho}_{\min}$ have no structural significance and it can be considered void regions.

3.2. Sensitivity calculation

The sensitivity analysis gives the gradients for the objective function and constraints in relation to design variables ρ^e. The direct methods are applied to obtain these sensitivities (Haftka *et al.*, 1990), and they are determinate using the equilibrium equations to Section 2, thus:

$$\frac{d\mathbf{u}_{out}}{d\rho^e} = \mathbf{L}_1^T \frac{d\mathbf{U}_2}{d\rho^e} \tag{11}$$

where, $\mathbf{L}_1^T$ is a vector consisting of zeros except for the position i, corresponding to the *d.o.f.* of the output direction, where its value is one. Deriving the Eq. (3) and (8) are obtained the terms $d\mathbf{U}_2/d\rho^e$ and $d\mathbf{P}_2/d\rho^e$, and using the Eq. (11):

$$\frac{d\mathbf{u}_{out}}{d\rho^e} = \mathbf{L}_1^T \mathbf{K}_2^{-1}\left\{\frac{\partial \mathbf{P}_2}{\partial \mathbf{U}_1}\frac{d\mathbf{U}_1}{d\rho^e} + \frac{\partial \mathbf{P}_2}{\partial \rho^e} - \frac{d\mathbf{K}_2}{d\rho^e}\mathbf{U}_2\right\} \tag{12}$$

now, deriving the Eq. (2) and (7) and using the Eq. (12) is obtained:

$$\frac{d\mathbf{u}_{out}}{d\rho^e} = \mathbf{L}_1^T \mathbf{K}_2^{-1}\left\{\frac{\partial \mathbf{P}_2}{\partial \mathbf{U}_1}\mathbf{K}_1^{-1}\left[\frac{\partial \mathbf{P}_1}{\partial \mathbf{U}_0}\frac{d\mathbf{U}_0}{d\rho^e} + \frac{\partial \mathbf{P}_1}{\partial \rho^e} - \frac{d\mathbf{K}_1}{d\rho^e}\mathbf{U}_1\right] + \frac{\partial \mathbf{P}_2}{\partial \rho^e} - \frac{d\mathbf{K}_2}{d\rho^e}\mathbf{U}_2\right\} \tag{13}$$

and, deriving the term $d\mathbf{U}_0/d\rho^e$, see Eq. (1):

$$\frac{d\mathbf{u}_{out}}{d\rho^e} = \mathbf{L}_1^T \mathbf{K}_2^{-1}\left\{\frac{\partial \mathbf{P}_2}{\partial \mathbf{U}_1}\mathbf{K}_1^{-1}\left[\frac{\partial \mathbf{P}_1}{\partial \mathbf{U}_0}\mathbf{K}_0^{-1}\left(\frac{d\mathbf{P}_0}{d\rho^e} - \frac{d\mathbf{K}_0}{d\rho^e}\mathbf{U}_0\right) + \frac{\partial \mathbf{P}_1}{\partial \rho^e} - \frac{d\mathbf{K}_1}{d\rho^e}\mathbf{U}_1\right] + \frac{\partial \mathbf{P}_2}{\partial \rho^e} - \frac{d\mathbf{K}_2}{d\rho^e}\mathbf{U}_2\right\} \tag{14}$$

finally, simplifying the Eq. (14):

$$\frac{d\mathbf{u}_{out}}{d\rho^e} = \boldsymbol{\Lambda}_0^T\left(\frac{d\mathbf{P}_0}{d\rho^i} - \frac{d\mathbf{K}_0}{d\rho^i}\mathbf{U}_0\right) + \boldsymbol{\Lambda}_1^T\left(\frac{d\mathbf{P}_1}{d\rho^i} - \frac{d\mathbf{K}_1}{d\rho^i}\mathbf{U}_1\right) + \boldsymbol{\Lambda}_2^T\left(\frac{d\mathbf{P}_2}{d\rho^i} - \frac{d\mathbf{K}_2}{d\rho^i}\mathbf{U}_2\right) \tag{15}$$

where:

$$\boldsymbol{\Lambda}_2 = \boldsymbol{L}_1^T \boldsymbol{K}_2^{-1} ; \qquad \boldsymbol{\Lambda}_1 = \boldsymbol{\Lambda}_2 \frac{\partial \boldsymbol{P}_2}{\partial \boldsymbol{U}_1} \boldsymbol{K}_1^{-1} ; \qquad \boldsymbol{\Lambda}_0 = \boldsymbol{\Lambda}_1 \frac{\partial \boldsymbol{P}_1}{\partial \boldsymbol{U}_0} \boldsymbol{K}_0^{-1} \tag{16}$$

$\boldsymbol{\Lambda}_0$, $\boldsymbol{\Lambda}_1$ (vectors n) and $\boldsymbol{\Lambda}_2$ (vector $2n$) are adjoint vectors. The sensitivity analysis is obtaining for each degree of freedom of the electrothermomechanical MEMS, thus we determine *d.o.f.* sensitivity analysis.

3.3. Numerical implementation

The Fig. 3 shows a flow chart of the optimization algorithm. Initially, the initial domain is discretized by finite elements and the designs variables are defined with the density ρ^e, which can assume different values in each finite element. The initial guess for design variables ρ^e consists of uniform values.

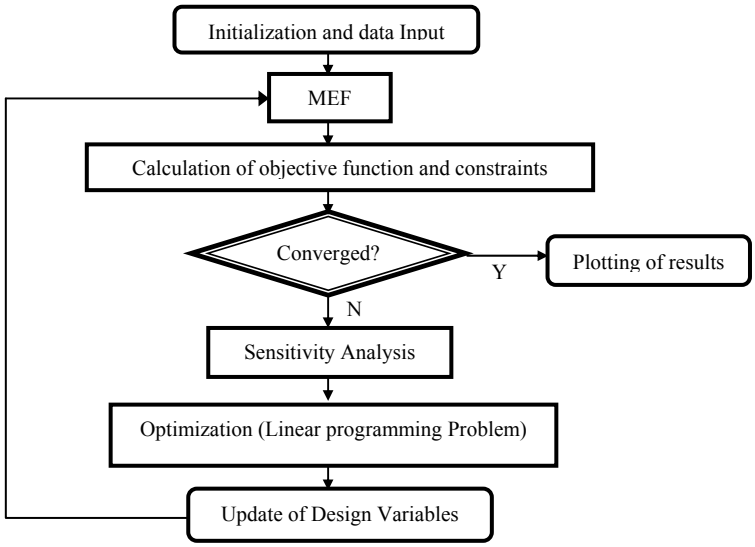

Figure 3. Flow chart of the optimization procedure.

In this work, the mathematical programming method (SLP) is applied to solve the linear programming (Haftka *et al.*, 1990). It consists of the sequential solution of approximation linear subproblems that can be defined by writing a Taylor series expansion for the non-linear problem – shown in Eq. (10), around the current design point ρ^e in each iteration step. This linearization requires the sensitivities (gradients) of the objective function – see Eq. (15) and (16).

In each iteration, moving limits are defined for the design variables. Typically, during the iterative process, the design variables will be allowed change by 5–15% of the original values. After linear optimization, a new set of design variables ρ^e is obtained and updated in the design domain until convergence is achieved for the objective function – the procedure has converged when the changes in design variables from iteration to iteration are below then 10^{-3}.

To avoid the traditional mesh dependency and checkerboard (regions with alternating solid and void element) problems in topology optimization (see Díaz and Sigmund, (1995) for a review) a filter was implemented. In this work, here we are used the Cardoso-Fonseca filter (Cardoso and Fonseca, 1999) that calculates the upper and lower bounds of the design variable ρ^e based on the design variable values of neighboring elements, avoiding strong material gradients inside of the domain. The amount of neighboring elements considered in the calculation is defined by specifying a radius. The Cardoso-Fonseca filter is applied to the moving limits of the design variables. This filter minimizes the dependence of the final result on the mesh refinement of finite element.

Since the electrothermomechanical MEMS topological problem is highly non-convex, the final topologies are obtained using the continuation method (Bendsøe and Sigmund, 2003) where the coefficients penalization p_1, p_2 varies from 1 to 2 and the elastic coefficient penalization p_3 varies from 1 to 3, with increment of 0,1 by iteration. The continuation method minimizes the problem of the local maximum multiples, allowing the topology optimization method to find a solution next to the global maximum.

4. Results

Two microactuators are presented to illustrate the capability of the program to design compliant micromechanisms actuated electro-thermally. The subsequent two examples include results changing the mesh refinement of finite element, and the material volume constraint. The data for the examples assumed nickel as material. This material property data and other useful data for topology optimization are shown in Tab. 1. In all examples we use a filter radius of eight neighboring elements.

Table 1. Material properties and topology optimization data used in the numerical examples

Description	Value
Electrical Conductivity (1/ohm.m)	6.4×10^{6}
Thermal conductivity (W/m ^{o}K)	90.7
Young's modulus (Pa)	2×10^{11}
Poisson's modulus	0.31
Thermal expansion coefficient (1/ ^{o}K)	15×10^{-6}
Heat transfer coefficient (W/m^{2} ^{o}K)	18.7×10^{3}
Environment temperature (^{o}K)	300
Volume constraint (%)	30
Initial guess for design variables	0.5
Spring of stiffness *K* (N/m)	1000

The design domains for a microactuator and a microgripper are shown in Fig. 4a and 4b, respectively, and the dimensions of the design domains (in micrometers), the electrical and mechanical boundary conditions (we assume environmental temperature in the mechanical supports points) and the electric potential applied. The first design domain is discretized by 2000 finite elements and the second by 3500 finite elements. The non-intuitive final topologies without filter are shown in Fig. 5a and 7a, respectively, and deformed final topologies simulated by finite element program ANSYS with the temperature distribution are shown in Fig.5b and 7b, respectively. The Fig. 5c sketches the historical for the material volume constraint, and the Fig. 7c shows the convergence curve for objective function.

The checkerboard problem in first and second design problems is removed in the final topologies using a filter, as shown in Fig. 6a and 8a. The deformed topologies and temperature distribution for these cases are sketched in Fig. 6b and 8b.

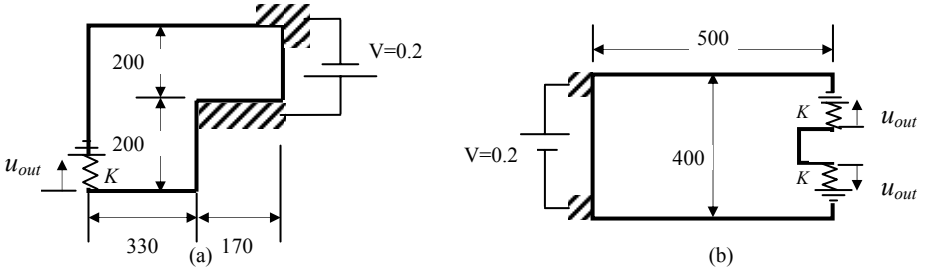

Figure 4. Design domains (thickness = 15μm). a) for a microactuator; b) for a microgripper.

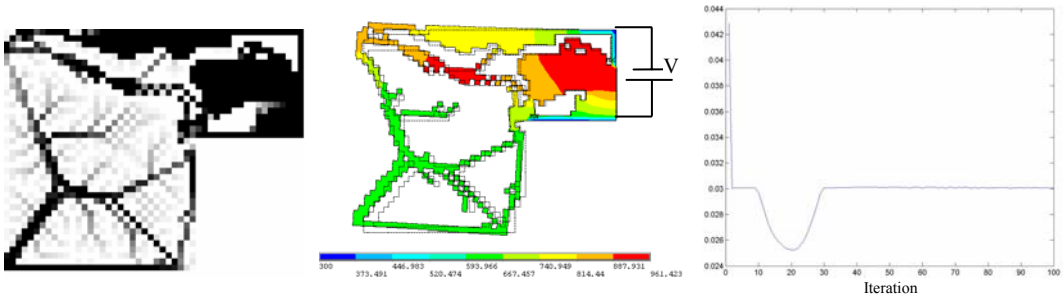

Figure 5. Result of the problem 5(a) without filter. a) Optimal topology; b) Displacement and temperature distribution; c) Convergence curve for the volume constraint.

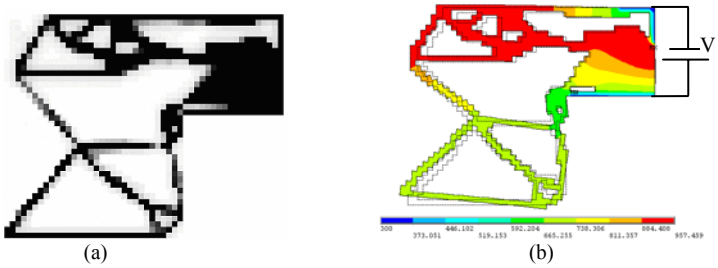

Figure 6. Result of the problem 5(a) with filter. a) Final topology; b) Displacement and temperature distribution.

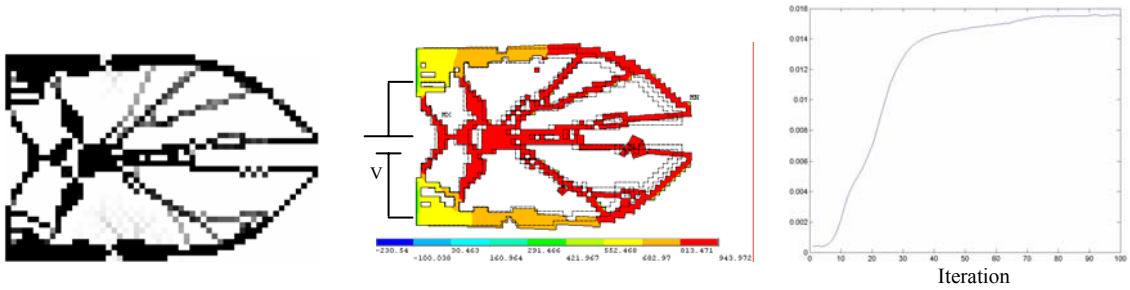

Figure 7. Result of the problem 5(b) without filter. a) Optimal topology; b) Displacement and temperature distribution; c) Convergence curve for the objective function.

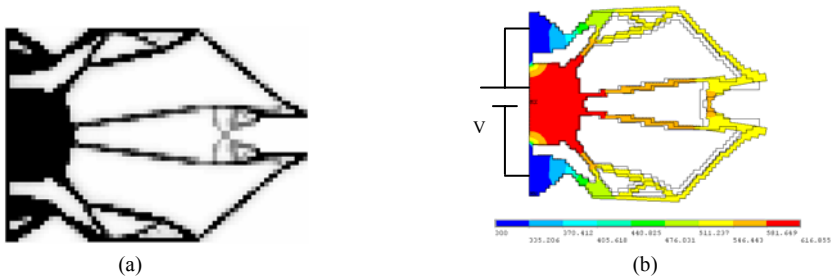

Figure 8. Result of the problem 5(b) with filter. a) Final topology; b) Displacement and temperature distribution.

In the Fig. 9 are employed several material volume constraints (15%, 30 and 50%). Though always the material distribution in the design domain converges to similar topologies, the optimal configuration is modifying according to material quantity available. Finally, the first row in Fig. 10 shows the influence of the mesh refinement in the final topologies for the problem sketched in Fig. 4b, without filter. In addition, the second row in Fig. 10 shows the influence in the final topology when the Cardoso-Fonseca filter is used for the same problem. The design domains are discretized by 500, 1800, and 3500 finite elements. Where no-filter is used we observe the rise of the checkerboard problem and a strong mesh dependency of the optimal solution when the mesh refinement is incremented. On the contrary, the Cardoso-Fonseca filter reduces these two problems.

Figure 9. Influence of the material volume constraint in the final topology.

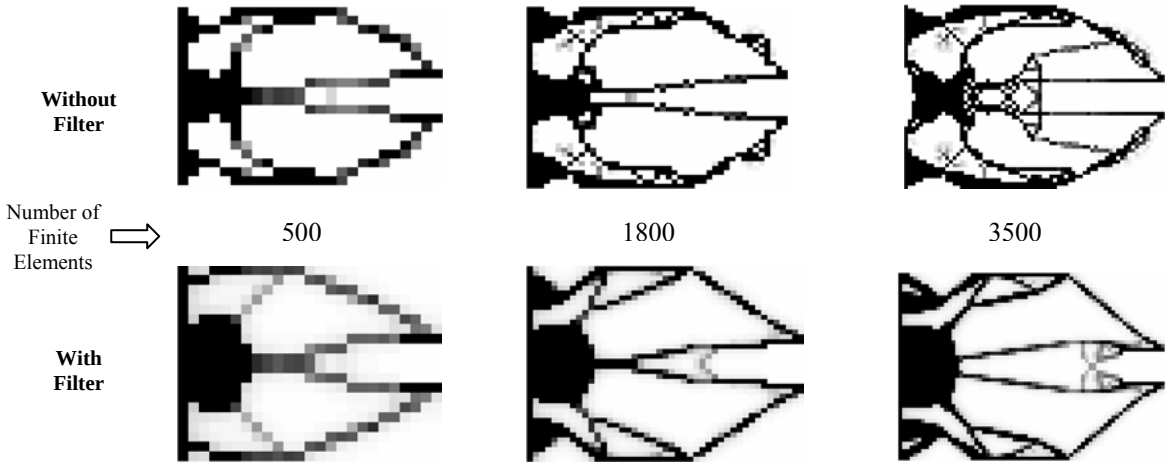

Figure 10. Influence of the mesh refinement in the optimal topology; without filter and with filter.

5. Conclusions

This work shows that topology optimization can be successfully applied as systematic tool to design compliant micromechanisms actuated electro-thermally. The optimization problem was defined as a design of a compliant mechanism considering the output load by a spring, which allows full control of the input-output behavior. Thus, several microactuators were achieved using topology optimization method based on SIMP and defining the design variables on each element finite. The microactuators fulfill the boundary conditions and the kinematics requirements by maximizing the desired output displacement.

As a future work, designs of other types of electrothermomechanical MEMS can be considered and prototypes will be manufactured and tested.

6. Acknowledgments

All authors thank FAPESP – São Paulo State Foundation Research Agency, for supporting him.

7. References

Ananthasuresh, G. K., 2003 "Optimal Synthesis Methods for MEMS", *Kluwer Academic Publishers*, Boston, 336p.

Bendsøe, M. P., Sigmund, O., 2003, "Topology Optimization: theory, Methods and applications", *Springer*, Berlin, 370p.

Bendsøe, M. P. and Sigmund, O, 1999, "Material Interpolations in Topology Optimization," *Arch. Appl. Mech*., Vol. 69, pp. 635-654.

Bendsøe, M. P., Kikuchi, N., 1988, "Generating Optimal Topologies in Structural Design Using a Homogenization Method". *Computer Methods in Applied Mechanics and Engineering*, Vol.71, pp.197-224.

Cardoso, E. and Fonseca, J., 1999, "Spatial gradient control in the structural topology optimization" in *Proceedings of First ASMO UK_ISSMO Conference on Engineering Design Optimization*.

Chen, R. S., Kung, C., Lee, G., 2002, "Analysis of the optimal dimension on the electrothermal microactuator", *J. Micromech. Microeng*., n.12, pp.291–296.

Chu, L. L., Gianchandani, Y. B., 2003, "A micromachined 2D positioner with electrothermal actuation and sub-nanometer capacitive sensing", *J. Micromech. Microeng*., n.13 pp.279–285.

Comtois, J. H., Michalicek, A, Barron, C. C., 1998, "Electrothermal actuators fabricated in four-lever planarized surface micromachined polycrystalline silicon"; *Sensors and Actuators A*, Vol.70, pp.23-31.

Díaz, A. and Sigmund, O., 1995, "Checkerboard Patterns in Layout Optimization", *Structural Optimization*, Vol.10, pp. 40-45.

Guckel, H., Klein, J., Christenson, T., Skrobis, K., Laudon, M., and Lovell, E. G., 1992, "Thermo-magnetic metal flexure actuators" *IEEE Solid-State Sensors and Actuators Workshop 5th*, pp.73–5.

Haftka, R. T., Gürdal, Z., Kamat, M. P., 1990, "Element of Structural Optimization", *Kluwer Academic Publishers*.

Howell, L. L., 2001, "Compliant Mechanisms", *John Wiley & Sons, Inc.*, New York, 459p.

Jonsmann, J., 1999, "Technology development for topology optimized thermal microactuators". Thesis (PhD), The Microelectronics Center, Technical University of Denmark, 116p.

Larsen, U. D., Sigmund, O, and Bouwstra, S., 1997, "Design and Fabrication of Compliant Micromechanisms and Structures with Negative Poisson's Ratio", *Journal of Microelectromechanical Systems*, Vol.6, n.2, pp.99–106.

Lintel, V. H., Pol, V. F., Bouwstra, S., 1988, "A piezoelectric micropump based on micromachining of Silicon", *Sensors and Actuators*, Vol.15, pp.153 – 160.

Mankame, N. D., Ananthasuresh, G. K., 2001, "Comprehensive thermal modeling and characterization of an electro-thermal-compliant microactuator", *J. Micromech. MicroEng*., Vol.11, pp.452-462.

Moulton, T., Ananthasuresh, G. K., 2000, "Micromechanical devices with embedded electro-thermal-compliant actuation", *Sensors and Actuators A*, Vol.90, pp.38-48.

Nishiwaki, S.; Min, S. J.; Yoo, J.; Kikuchi, N., 2001, "Optimal structural design considering flexibility", *Comput. Methods Appl. Mech. Engrg.*, Vol.190, pp. 4457-4504.

Rubio, M. W., Souza, B. R. D., and Silva, E. C. N., 2004, "Projeto de microsistemas eletrotermomecânicos utilizando otimização topológica". *Proceedings CBA 2004*, (CD-ROM).

Silva, E. C. N., Fonseca, J. S. O., Kikuchi, N., 1997, "Optimal design of piezoelectric microstructures", *Computer Methods in Applied Mechanics and Engineering*, Vol.159 n.2, pp.49-77.

Sigmund, O., 2001a, "Design of Multiphysics Actuators Using Topology Optimization – Part I: One-material Structures", *Computer Methods in Applied Mechanics and Engineering*, Vol.190, pp.6577-6604.

Sigmund, O., 2001b, "Design of Multiphysics Actuators Using Topology Optimization – Part II: Two-material Structures", *Computer Methods in Applied Mechanics and Engineering*, Vol.190, pp.6605-6627.

8. Responsibility notice

The authors are the only responsible for the printed material included in this paper.